International Forum on Aeroelasticity and Structural Dynamics
IFASD 2019
10-13 June 2019, Savannah, Georgia, USA

CONTROL SURFACE MODELLING OF UNSTEADY LARGE AMPLITUDE MOTION VIA CHIMERA CFD TECHNIQUE

Bernd Stickan[1], **Reik Thormann**[1], **Hans Bleecke**[1]

[1]Airbus Operations GmbH
Department of Aeroelasticity
Bernd.B.Stickan@airbus.com

Keywords: CFD, Chimera, Overlap, Overset, Unsteady CFD, Control Surfaces

Abstract: Computation Fluid Dynamics (CFD) are used for the generation of unsteady aerodynamic models for dynamic computations like flutter and gust load analysis. For both application fields, the accurate prediction of control surface aerodynamics is of major importance. The presented study focusses on motion with relatively large amplitude to analyze unsteady nonlinear effects. To model this effect accurately, the Chimera/overlap grid technique is used. This CFD technique uses different mesh blocks with overlap areas. The overlap areas are used to interpolate the fluid quantities (e.g. density, pressure and velocity) between the blocks. For the here investigated control surface nonlinearities, the influence of the control surface gaps on the unsteady aerodynamic forces as a result of forced motion is analyzed.

Starting point is the investigation of the gap-influence on steady results by comparing Chimera to a workaround solution, which applies mesh deformation including a blending area to allow large amplitude motion, rather than modeling the gap.

The unsteady part starts with a first validation by comparing results with Chimera and with the workaround solution for very small amplitudes. Aerodynamic forces are analyzed thereafter for different motion amplitudes. Results are compared to the workaround solution. The influence of the unsteady control surface nonlinearities under large amplitudes is of particular importance for the simulation of gust load alleviation functions and limit cycle oscillations.

1 INTRODUCTION

CFD can be used for the calculation of unsteady aerodynamic frequency-domain data needed for flutter and gust-load computations, see [1] and [2]. The used frequency domain models are unsteady linear models, nonlinear effects are not taken into account. But CFD allows also to model unsteady nonlinear effects, see [3].

The accurate modeling of control surface is a very important task for the creation of unsteady aeroelastic aircraft models. To also correctly consider nonlinear effects for control surfaces, the present paper analyzes if the common way of working for control surface movement as seen in Figure 1, left, is of adequate accuracy or if geometrically more detailed control surface modelling employing the CFD Chimera technique is required, see 1, right.

The first approach is neglecting the gap between control surface and the main wing structure, which opens when the control surface is rotated out of the zero-degree position. The closure of

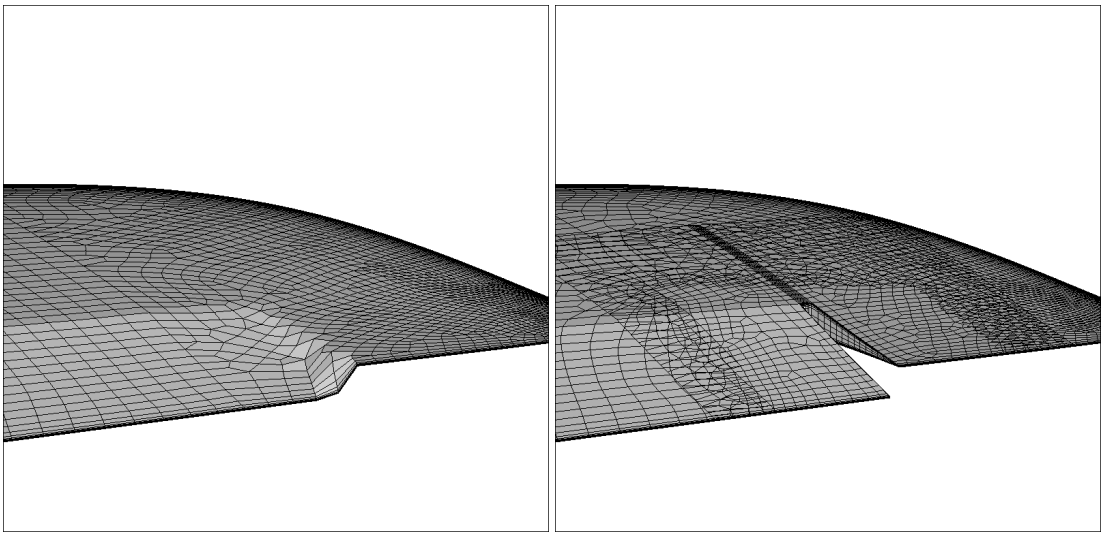

Figure 1: Control surface movement via surface blending (left) or with Chimera method (right)

the CFD-surface for a rotating control surface is established through a transition area in which the control surface movement is smeared over a certain blending distance.

The second approach uses the Chimera mesh overset method to model the gap correctly. This special technique allows to rotate the control surface with an accurate gap geometry. For this technique different CFD mesh blocks must be created which fulfill the requirements of the CFD solver for the accurate interpolation between the mesh blocks, see [4]. Accordingly, this approach is more challenging in terms of mesh generation and mesh deformation.

For both ways of working the hinge-line area is handled through mesh deformation, so no gap is modeled there.

2 METHODS

The DLR TAU-code is applied to solve the steady and the unsteady Reynolds Averaged Navier Stokes (URANS) equations [5]. The solver is working with a cell-vertex-based finite volume scheme on unstructured grids. In the following studies the Spalart-Allmaras model [6] is used. The focus of this work is the usage of the Chimera technique in the TAU code, see [7]. It is often also referred as mesh overset method. Some application examples for the usage of TAU with the Chimera technique for the modeling of control surfaces are presented in [4] and [8].

The unsteady aerodynamics are generated by a forced, harmonic oscillation of the CFD mesh. For the deformation of the CFD mesh, radial basis function interpolation with a nearest-surface point correction step is applied. The time-history of the pressures is used to compute the unsteady pressure transfer function $\widehat{cp}$, see further details in [3] and [9]. An additional deformation step has been added here to protect the sensitive Chimera overlap areas.

Figure 2 shows as example the monitored C-lift and Generalized Air Forces (GAF) in the first row for a harmonic control surface excitation. Below are the online computed frequency domain outputs in magnitude and phase. These are the transfer function with C-lift/GAF as output signal and the control-surface angle as input signal. When these values reach a certain convergence limit, the simulation is finished.

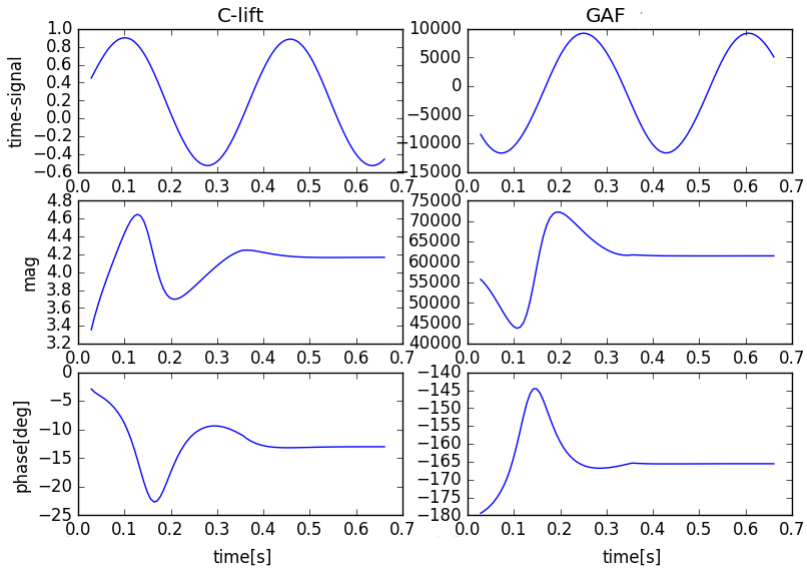

Figure 2: Online-monitoring example of time-domain simulation with harmonically moving control surface, transfer function (shown in mag(nitude) and phase) computed with moving analysis window

3 MESH

As already indicated, the mesh creation is a demanding first step towards unsteady simulations with the Chimera CFD technique. Starting point is the background mesh as seen in Figure 3. This mesh models the clean wing geometry without any control surface details. The same grid can also be used for the pure mesh deformation approach, which does not resolve the control surface gaps. For the following simulations, the background mesh is expanded with 2 further mesh blocks which are visible in Figure 4. The right plot highlights the overlap of the two additional mesh blocks. It shows also that the boundary layer is not modeled accurately in the gap itself to ease the overall process. The size of the gap is approximately 0.4 percent of the span. Moreover, the figure shows that the Chimera technique is not used to model the complete control surface, but only the outer gap of an elevator. The inner end of the elevator is only modeled with the mesh blending approach, see Figure 5.

4 STEADY RESULTS

To validate the Chimera results a first point has been computed for a control surface deflection angle of $\alpha_{CS} = 1°$ for both modeling approaches for Mach=0.7. The result is presented in Figure 6. This and the following plots show the surface delta-pressure Δcp, which is the difference of pressures for the deflected case and the undeflected $\alpha_{CS} = 0°$ case. While the span stations further away from the gap location show an excellent agreement between both mesh, small differences are visible close to the gap location.

Figure 7 shows the same comparison for a $\alpha_{CS} = 13°$ deflected control surface. It can be noted that close to the gap at eta≈1 differences between the two approaches have increased compared to the $\alpha_{CS} = 1°$ result. The gap-resolving Chimera solution produces more lift on the control surface close to the gap. Further away from the gap for eta=0.8, differences are not visible any more. The overall flow characteristics can be observed in Figure 8. The main flow characteristics are apparently not differing between the two modeling approaches.

Another flow feature comparison for the gap area can be seen for $\alpha_{CS} = -10.5°$ and Mach=0.85 in Figure 10. Here the differences in the flow-features are bigger, since the Chimera result shows

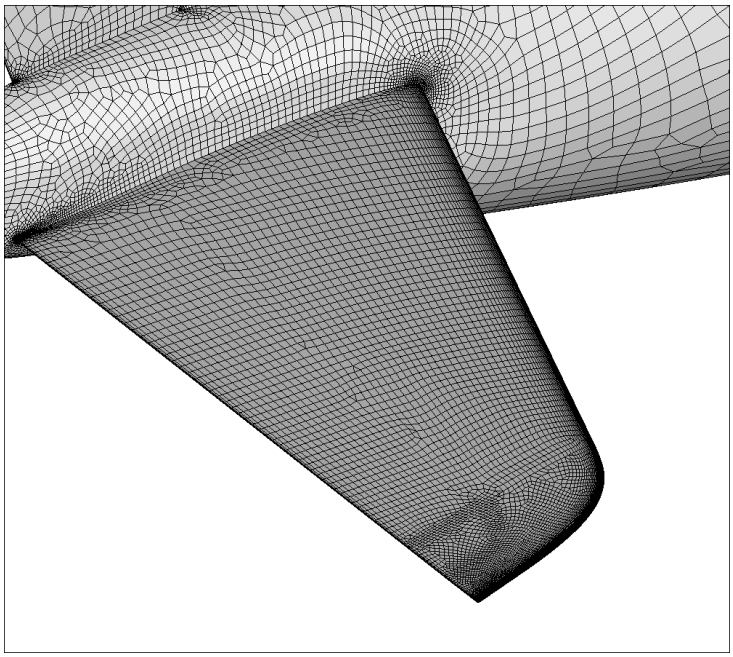

Figure 3: Background mesh

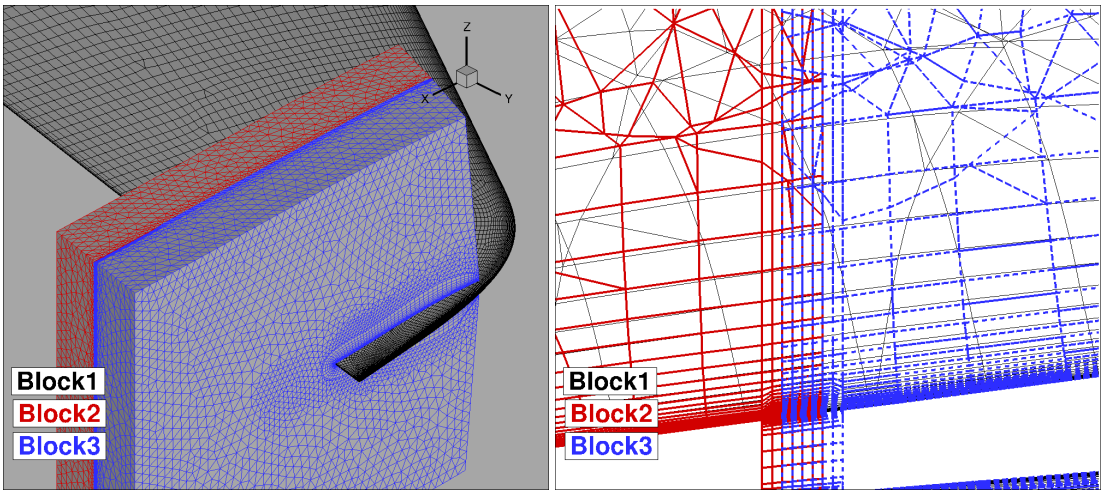

Figure 4: Background mesh: left - overview, right - volume cut with cut-plane normal in flow direction

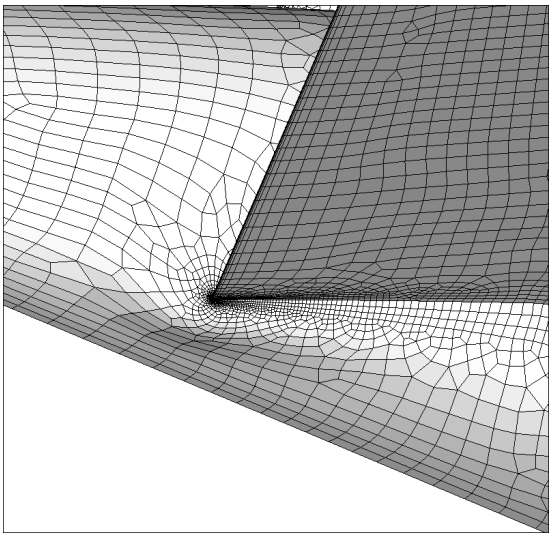

Figure 5: Modeling of inner control surface intersection with fuselage via surface blending

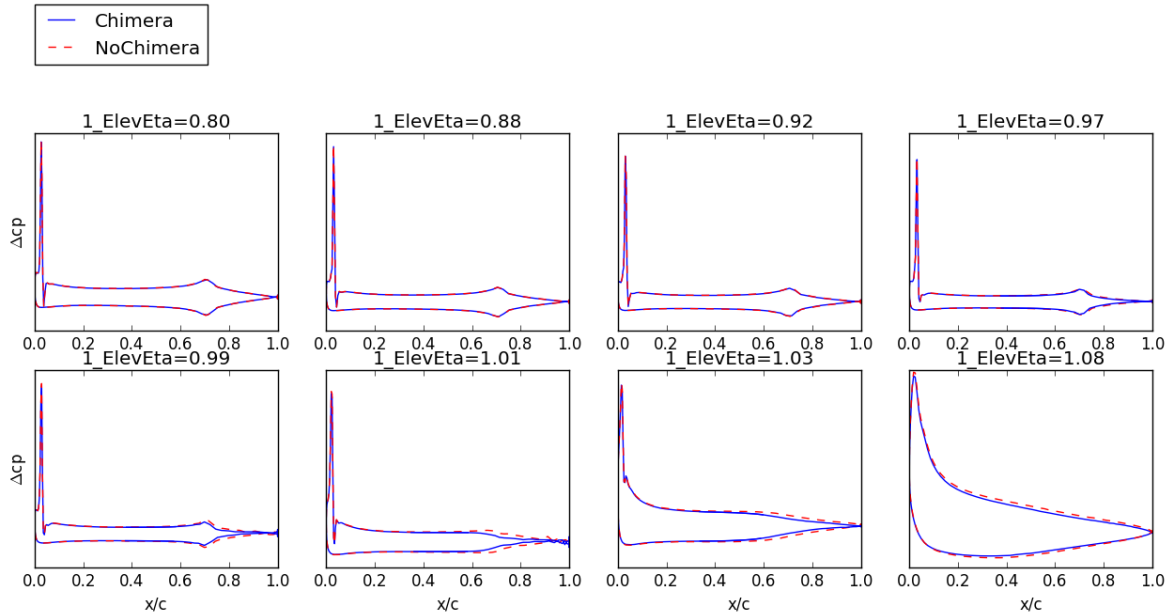

Figure 6: Steady delta pressures for control-surface angle = 13 deg. minus control-surface angle = 0 deg, Mach=0.7, altitude=30.000 feet, eta=1 is location of gap

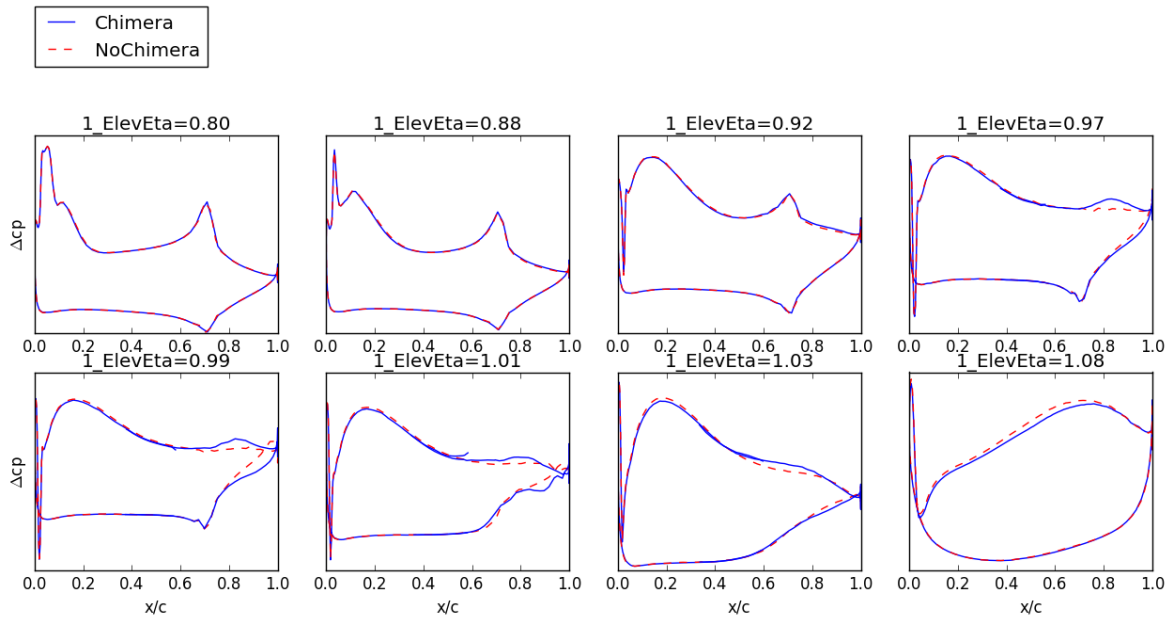

Figure 7: Steady delta pressures for control-surface angle = 13 deg. minus control-surface angle = 0 deg, Mach=0.7, altitude=30.000 feet, eta=1 is location of gap

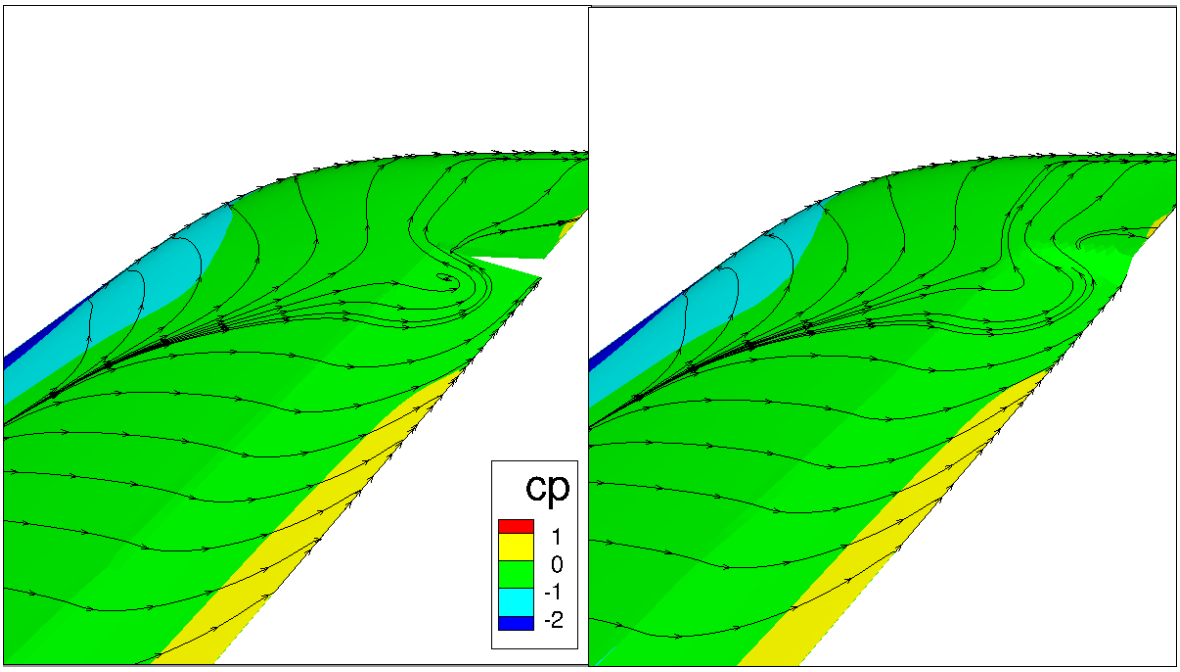

Figure 8: Surface solution, steady pressure and skin-friction lines for Chimera mesh (left) and regular mesh (right), Mach=0.7, control-surface angle=13.0deg

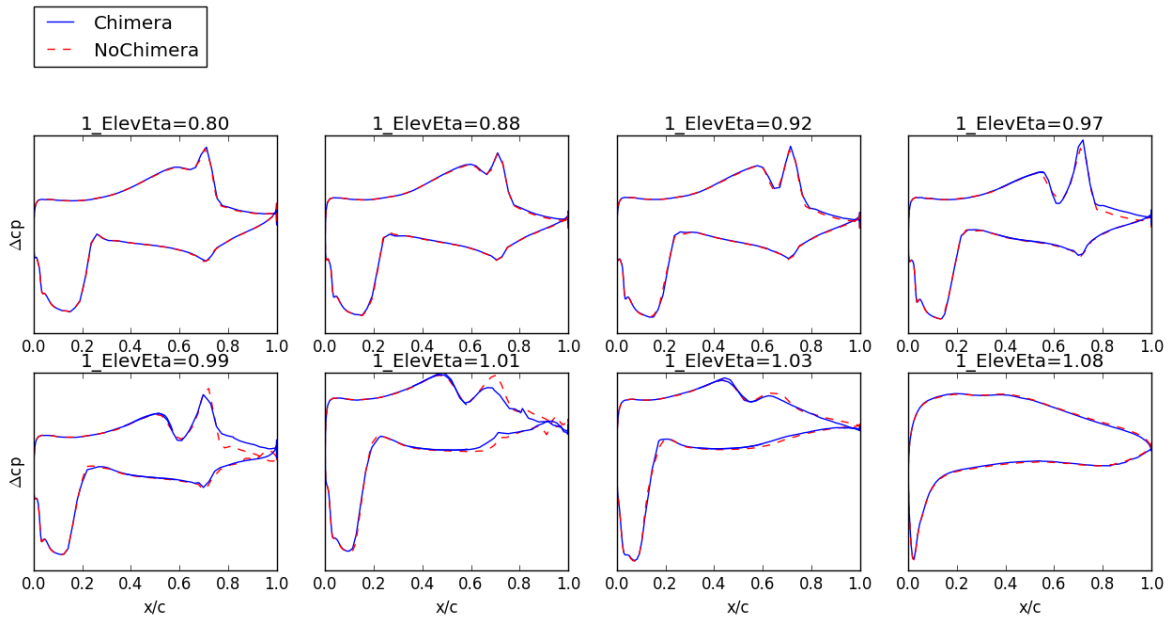

Figure 9: Steady delta pressures for control-surface angle =-10.5 deg. minus control-surface angle = 0 deg, Mach=0.85, altitude=30.000 feet, eta=1 is location of gap

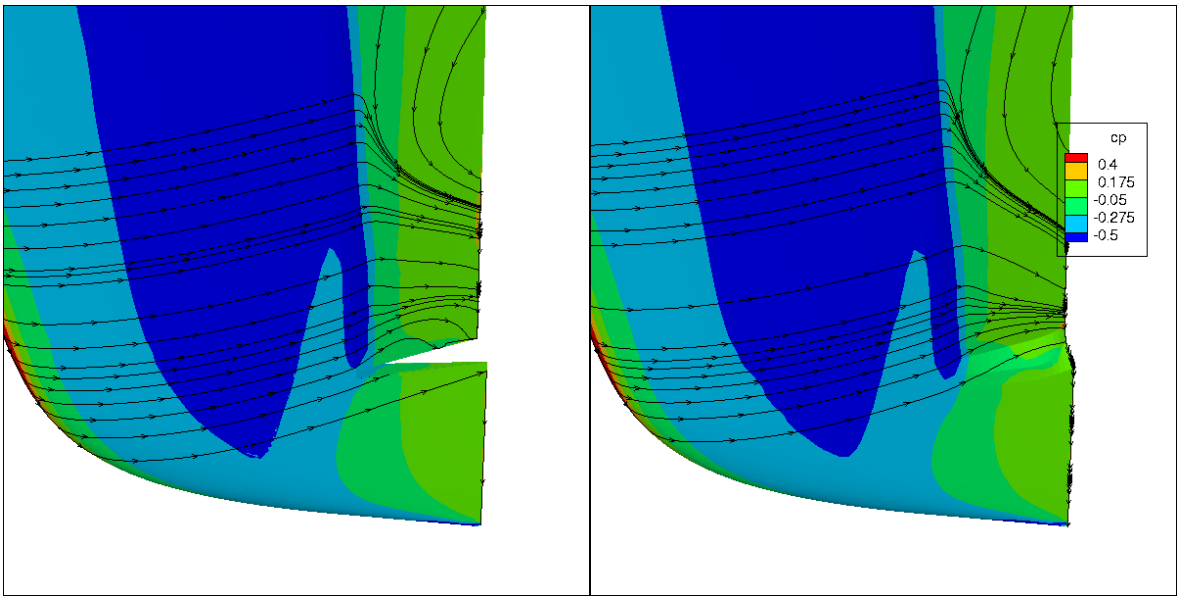

Figure 10: Surface solution, steady pressure and skin-friction lines for Chimera mesh (left) and regular mesh (right), Mach=0.85, control-surface angle=-10.5

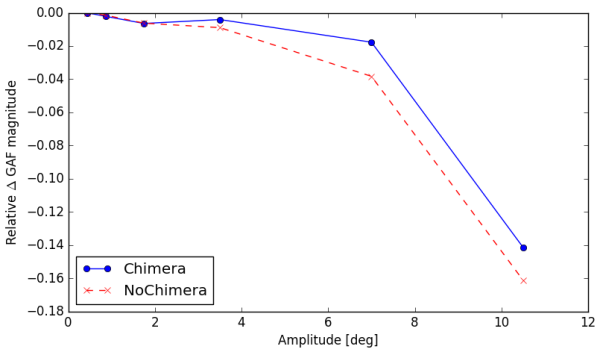

Figure 11: Nonlinear effects on Generalized Air Force for red. freq. k=0: excitation of first bending mode by control surface rotation, Mach=0.85, altitude=30.000 feet

clearly a ‘leakage’ through the gap. This leads to slightly increased differences in for the delta-pressures presented in Figure 9. The global amplitude effect is visible in Figure 11. The plot shows the nonlinear change in the amplitude-normalized generalized air forces acting on the first bending mode by the control surface rotation. Further details are explained in Section 5. The global effect is not very different between the two control surface modeling approaches.

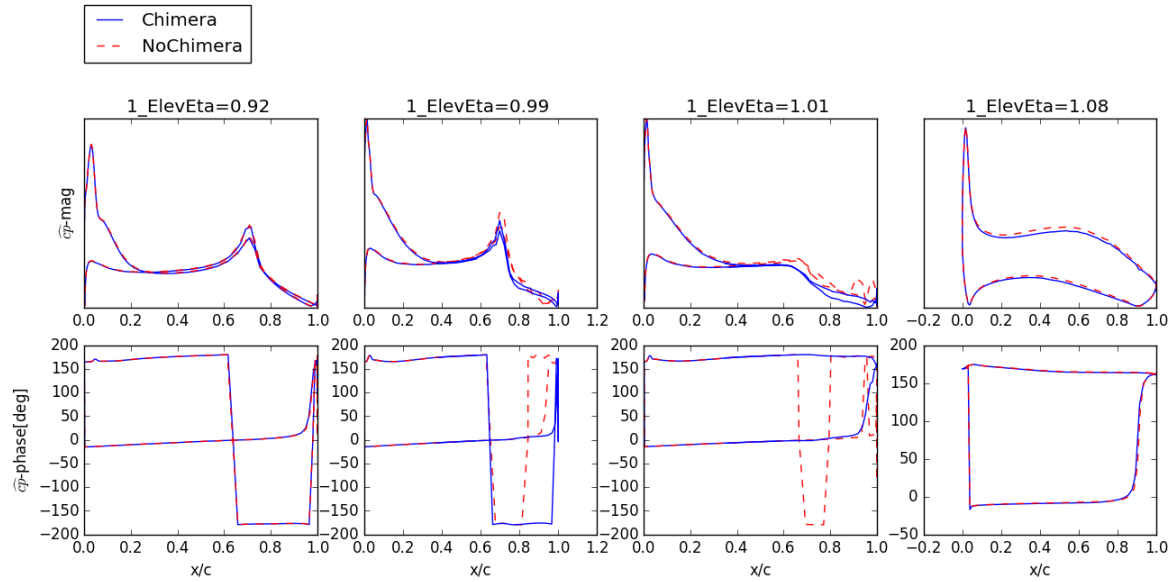

Figure 12: Unsteady surface pressure for red. freq. k=0.1 due to control surface mode, amplitude=10.5, Mach=0.7, altitude=30.000 feet

5 UNSTEADY RESULTS

The steady conditions were used as starting point for unsteady simulations with a rotating control surface. Figure 12 shows unsteady surface pressures $\widehat{cp}$, the complex-valued pressure transfer function due to the control surface movement. Here the magnitude effect differences between the two method seems to cancel out between upper and lower wing side.

Figure 13 compares for the 2 different reduced frequencies the unsteady nonlinear effects due to the motion amplitude. For this purpose the Generalized Air Force

$$\text{GAF} = \boldsymbol{\phi_i^T} \cdot \boldsymbol{n} \cdot \boldsymbol{a} \cdot \widehat{cp}\,(\boldsymbol{\phi_j}) \tag{1}$$

is computed for $\boldsymbol{\phi_i}$ equal to the first-bending mode. $\boldsymbol{\phi_j}$ denotes the control-surface rotation mode. The surface normal and surface cells size are defined by $\boldsymbol{n}$ and $\boldsymbol{a}$, respectively. The first bending mode has been selected to weight the outer wing aerodynamics stronger in the resulting values. The nonlinearities are larger for the non-Chimera approach. Furthermore, the nonlinear magnitude effect decreases with increasing amplitude. The delta in phase does not give a clear picture, but it should be noted that the values are below the selected accuracy of the nonlinear harmonic motion simulation. So it might be the case that the CFD excitation time was not sufficient.

Figure 14 shows unsteady surface pressure for the largest investigated amplitude for Mach=0.85. In this case the transonic shock movement, which leads to the big magnitude hill of $\widehat{cp}$, dominates the unsteady pressures. The effects close the gap-location are similar to Figure 12 for Mach=0.7.

Figure 15 compares the nonlinear effects in the GAF for the 2 different reduced frequencies at Mach=0.85. As for the previous analyses, the nonlinear effects decrease with increasing reduced frequency. Probably, dynamic-overshoot effects reduce the influence of the gap modeling. Secondly, the nonlinear effects are larger in this case for the surface-blending solution, although the differences are not very big.

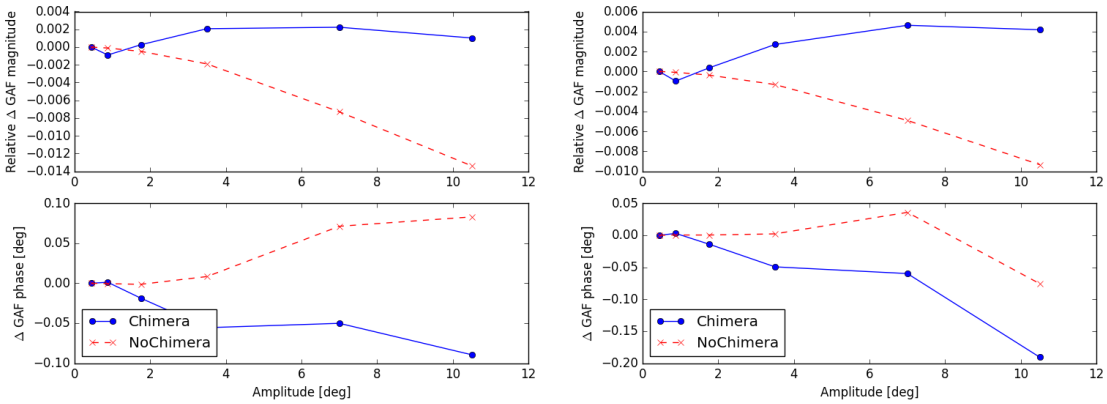

(a) $k = 0.1$ (b) $k = 0.3$

Figure 13: Nonlinear effects on Generalized Air Force for different reduced freq. k: excitation of first bending mode by control surface rotation, Mach=0.7, altitude=30.000 feet

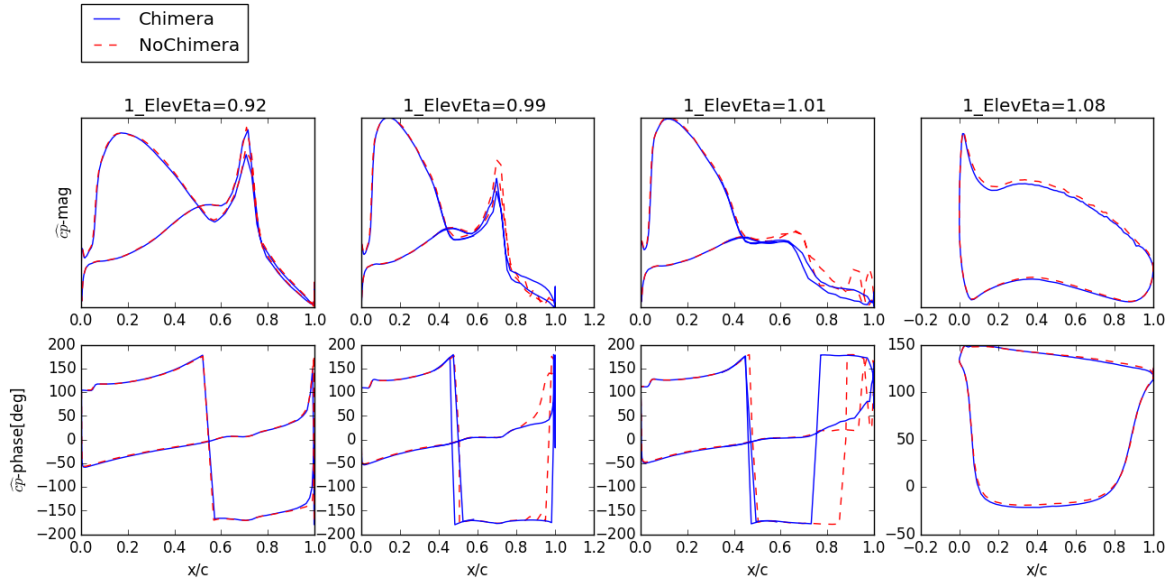

Figure 14: Unsteady surface pressure for red. freq. k=0.3 due to control surface mode, amplitude=10.5, Mach=0.85, altitude=30.000 feet

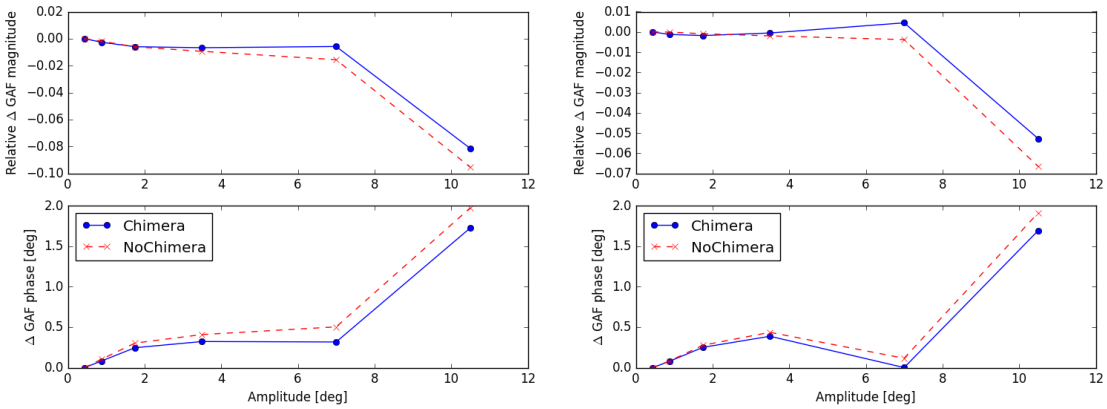

(a) $k = 0.1$ (b) $k = 0.3$

Figure 15: Nonlinear effects on Generalized Air Force for different reduced freq. k: excitation of first bending mode by control surface rotation, Mach=0.85, altitude=30.000 feet

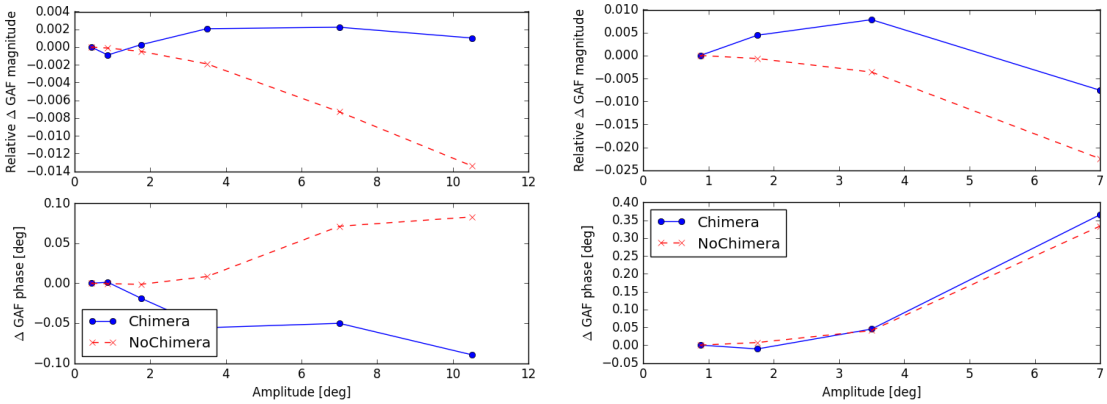

(a) $k = 0.1, \alpha_{CS,\text{static}} = 0°$ (b) $k = 0.1, \alpha_{CS,\text{static}} = -7°$

Figure 16: Nonlinear effects on Generalized Air Force for different static control surface angle $\alpha_{CS,\text{static}}$: excitation of first bending mode by control surface rotation, Mach=0.7, altitude=30.000 feet

Finally, Figure 16 compares the nonlinear effects for a mean/static control surface angle $\alpha_{CS,\text{static}}$ of zero and seven degree up. Here for both approaches, the nonlinear effects have increased for the non-zero mean position of the control surface.

6 CONCLUSION AND OUTLOOK

This document showed the usage of the Chimera CFD mesh overset technique for the modeling of control surfaces. The aim of the study was to analyze the influence on unsteady aerodynamic nonlinearities due to increasing motion amplitudes with modeling of the control surface gaps. For subsonic settings the Chimera and surface-blending solution did show a good agreement. The differences increased with increasing Mach-number. The nonlinear unsteady effects are relatively similar for both solutions. Larger nonlinear unsteady effects can be expected for smaller reduced frequencies. Additionally, larger nonlinear effects were visible for static, non-zero control-surface angles. Overall, the workaround solution through surface-deformation did show a good agreement to the gap-resolving Chimera results.

The here presented study should be enlarged to a wider parameter range, analyzing deeper the effects of Mach-number, static deflection angles, larger motion amplitudes. Furthermore, the application to spoiler aerodynamics is a necessary next step. In this case, the Chimera technique is indispensable to accomplish large spoiler amplitudes. Additionally, especially for even larger dynamic control surface angles, an inaccuracy of the current simulation must be removed: Currently the excitation input mode ϕ_j is only scaled to different amplitudes. This means the control surface chord length grows for large amplitudes. In the present study this effect is neglected for the dynamic motion.

7 REFERENCES

[1] Stickan, B., Schröder, F., Helm, S., et al. (2018). On recent advances in industrial high-fidelity aeroelasticity. In R. Heinrich (Ed.), *AeroStruct: Enable and Learn how to Integrate Flexibility in Design*, Notes on Numerical Fluid Mechanics and Multidisciplinary Design. Springer Berlin Heidelberg.

[2] Weigold, W., Stickan, B., Travieso-Alvarez, I., et al. (2017). Linearized unsteady cfd for gust loads with tau. In *IFASD 2017 - International Forum on Aeroelasticity and Structural Dynamics*.

[3] Stickan, B. (2018). *Explanation of AEROSTABIL limit-cycle oscillations via high-fidelity aeroelastic simulations*. Ph.D. thesis.

[4] Reimer, L. and Heinrich, R. (2013). *Modeling of Movable Control Surfaces and Atmospheric Effects*. Berlin, Heidelberg: Springer Berlin Heidelberg. ISBN 978-3-642-38877-4, pp. 183–206.

[5] Gerhold, T. and Galle, M. (1997). Calculation of complex three-dimensional configurations employing the DLR TAU-code. *AIAA Paper 97-0167*.

[6] Spalart, P. and Allmaras, S. R. (1992). A one-equation turbulence model for aerodynamic flows. AIAA Paper 92-0439.

[7] Madrane, A. (2006). Parallel implementation of a dynamic overset unstructured grid approach. In C. Groth and D. W. Zingg (Eds.), *Computational Fluid Dynamics 2004*. Berlin, Heidelberg: Springer Berlin Heidelberg. ISBN 978-3-540-31801-9, pp. 733–739.

[8] Capsada, L. A. and Heinrich, R. (2018). Development of the dlr tau code for modelling of control surfaces. In *Deutscher Luft- und Raumfahrtkongress*.

[9] Kaiser, C., Thormann, R., Dimitrov, D., et al. (2015). Time-linearized analysis of motion0induced and gust-induced airloads with the dlr tau code. In *Deutscher Luft- und Raumfahrtkongress*.

COPYRIGHT STATEMENT